HHS Public Access

Author manuscript

Br J Dermatol. Author manuscript; available in PMC 2015 July 17.

Published in final edited form as:

Br J Dermatol. 2014 July ; 171(1): 30–38. doi:10.1111/bjd.12899.

12/15-Lipoxygenase Deficiency Reduces Densities of Mesenchymal Stem Cells in the Dermis of Wounded and Unwounded Skin

S. Hong[#], **B.V. Alapure**[#], **Y. Lu**, **H. Tian**, and **Q. Wang**

Center of Neuroscience Excellence, Louisiana State University Health Science Center, New Orleans, LA 70112

[#] These authors contributed equally to this work.

Abstract

Background—Mesenchymal stem cells (MSCs) promote skin healing. 12/15-lipoxgenase (LOX) is crucial in producing specific lipid mediators in wounded skin. The consequences of 12/15-LOX deficiency (12/15-LOX$^{-/-}$) on MSC densities in skin are unknown.

Objectives—To determine the effect of 12/15-LOX$^{-/-}$ on MSC densities in the wounded and unwounded dermis.

Methods—Full-thickness skin incisional wounds were made to 12/15-LOX$^{-/-}$ and wildtype (WT) C57BL/6 mice. Wounded skin was collected at 3, 8, or 14 days post-wounding (dpw). MSCs were analyzed in skin sections via histology. 12*S*- or 15*S*-hydroxy-eicosatetraenoic acid (HETE) was analyzed using reversed-phase chiral liquid chromatography-ultra-violet spectrometer-tandem mass spectrometer.

Results—There were more Sca1^{+}CD29^{+}MSCs (cells/field) at 3, 8 and 14 dpw and more Sca1^{+}CD106^{+}MSCs at 3 and 14 dpw in the wounded dermis, and more MSCs in unwounded dermis of wildtype (WT) mice compared to 12/15-LOX$^{-/-}$ mice, and more MSCs in the wounded dermis than in the unwounded dermis. For 12/15-LOX$^{-/-}$ dermis, Sca1^{+}CD106^{+}MSCs peaked and Sca1^{+}CD29^{+} MSCs reached a flat level at 8 dpw. However for the WT dermis, MSCs increased from 8 to 14 dpw. There were more Sca1^{+}CD106^{+}MSCs than Sca1^{+}CD29^{+}MSCs in the 12/15-LOX$^{-/-}$ wounded dermis at 8 dpw. However, more Sca1^{+}CD29^{+}MSCs were in the 12/15-LOX$^{-/-}$ than Sca1^{+}CD106^{+}MSCs in the WT wounded dermis at 3 dpw and Sca1^{+}CD106^{+}MSCs and Sca1^{+}CD29^{+}MSCs were at comparable levels in other conditions. 12/15-LOX$^{-/-}$ suppressed levels of 12/15-LOX protein and their products 12*S*-HETE and 15*S*-HETE in wounds.

Conclusions—12/15-LOX$^{-/-}$ reduces MSC densities in dermis, which correlates with the suppressed 12/15-LOX pathways in wounded and unwounded skin.

Correspondence to Song Hong, LSUHSC -Center of Neuroscience Excellence, Lions Building, 2020 Gravier St., Suite D, New Orleans, LA 70112; Tel: 504 599-0838; Fax: 504 599-0891; shong@lsuhsc.edu..

Conflict of Interest Disclosures: none declared.

Keywords

12/15-Lipoxygenase; Mesenchymal Stem Cells; Skin dermis wounds; CD29, C106, Sca1; Stem cell density and homing

Introduction

12/15-lipoxygenase (LOX) is one of the key enzymes that catalyze the critical oxygenation for transformation of unsaturated essential fatty acids to lipid mediators in the skin[1–5]. These lipid mediators include anti-inflammatory and pro-resolving lipoxins, resolvins, and protectin/neuroprotectin D1[6–8]; anti-inflammatory oxygenated phospholipids[9,10] and 15*S*-hydroxy eicosatetraenoic acid (HETE)[11]; 14*S*,21*R*-dihydroxy docosahexaenoic acid (14*S*, 21*R*-diHDHA), which enhances the functions of mesenchymal stem cells (MSCs) in wound healing[2]; angiogenic 12*S*-HETE; and pro-inflammatory hepoxilins and trioxilins[12]. 12/15-LOX is induced in the skin by injury[5]. The essential role of 12/15-LOX in skin repair is indicated by the published evidence that12/15-LOX deficiency or knockout (12/15-LOX$^{-/-}$) suppresses wound repair[2,3,13,14], where the mechanisms are evolving and awaiting further delineation.

Many reports, including ours, show that mesenchymal stem cells (MSCs) promote wound healing[2,15–17]. Transplanted MSCs promote wound healing by producing paracrine angiogenic cytokines[2,18,19] and by possibly differentiating into skin cells[18–22]. densities of transplanted or endogenous MSCs in the dermis of wounded skin is a critical for MSC function in healing and homeostasis in skin [2,20,23]. MSCs express specific markers stem cell antigen (Sca1), CD29, and CD106, which in turn have been recognized as markers of MSC identification in many publications[24,25].

There are no reports to date regarding the role of LOXs in MSC densities in tissue or organs. We hypothesized that 12/15-LOX$^{-/-}$ reduces endogenous MSC densities in the wounded dermis because of the pro-healing actions of 12/15-LOX or MSCs[2], and in unwounded dermis as MSCs are likely to contribute to dermic homeostasis. This hypothesis was tested and evidenced here by determining the presence of MSCs in the wounded and unwounded dermis of 12/15-LOX$^{-/-}$ mice and their control using immunohistological methods.

Materials and methods

Incisional wound healing and sample collection

We used 12/15-LOX$^{-/-}$ and congenic WT (C57BL/6) control mice (10-wk-old, Jackson Lab). The protocol was approved by the Institutional Animal Care and Use Committee and Institutional Review Board of our institute. Mouse hair on the dorsal side was removed by Veet depilating cream. Two full-thickness incisions (20 mm length per incision) were made on the dorsal side symmetrically across the midline except for the sham mouse (which was not wounded). Incisions were closed with two sutures (Ethilon 6–0). The sutures were removed at 5 days post-wounding (dpw). The six mice in each group were perfused (5 ml/min, 5 min) via cardiac puncture with PBS$^{-/-}$ (without Ca^{2+} and magnesium) under anesthesia, then were killed; then skin around the incision (15 mm rim, or equivalent area

for sham), was collected at 3, 8, and 14 dpw (12 wounds/group). The skin samples were fixed in 4% paraformaldehyde (4 h, ~23°C), incubated in 30% sucrose (12 h, 4°C), and embedded in OCT for immunohistological analysis [1,26].

Hisotochemistry: hematoxylin and eosin staining and scanning microscope analysis of skin sections

Serial sagittal cryosections (7 μm thick) were prepared using a Leica CM3050s cryostat microtome and transferred to Superfrost slides, then stained with H&E as we did before[1–3]. The sections were processed sequentially as follows: incubated in PBS (5 min, ~23°C) to remove the OCT; dehydrated, stained with hematoxylin (2 min, ~23°C); rinsed with tap water to remove extra hematoxylin; quickly dipped through 1% HCl/alcohol then 0.3% ammonia water to enhance hematoxylin staining and remove extra hematoxylin; and incubated at ~23°C in 80% alcohol (10 sec) and then in 0.5% eosin (2 min). The sections dipped in 95% alcohol (6 times), 100% alcohol (3 times), and then xylene (3 times) to clean extra eosin, submerged in Crystate mounting media (Fisher), covered with coverslips and dried (~23°C), and then imaged using an Olympus scanning microscope. The images were analyzed via Olympus OlyVIA and Photoshop software.

Immunofluorescent histology

Skin cryosections (7μm thick) were incubated sequentially in the following: methanol/acetone (1/1) (20 min, −20°C); citrate buffer (20 min, 90–100°C); blocking buffer [5% Goat/Donkey serum and 0.3% trition-X-100; 1 hour, ~23°C]; two anti-mouse primary antibodies: Sca1 (host: rat; dilution 1:50; eBiosciences, San Diego, CA, USA) and CD29 or CD106 (host: rabbit; dilution 1:50;Santa Cruz biotech., San Diego, CA, USA), or an antibody of 12/15-LOX/Alox15 (host: rabbit; 1:50; Santa Cruz biotech.) (4°C, 12 h); and then one or two compatible secondary antibodies (anti-rat, AlexaFluor488; and anti-rabbit, AlexaFluor568; host: donkey). Nuclei were stained with DAPI to be fluorescent blue. Slides were imaged by a Zeiss deconvolution microscope. The co-stained MSCs were counted. Intensity summation of green pixels per high power field (HPF) of 12/15-LOX stained skin sections were measured using NIH Image J for 12/15-LOX quantification. Data were analyzed by Mann–Whitney Anova or t-test. A p-value of < 0.05 was considered statistically significant.

LC-UV-MS/MS analysis of typical lipid products representing 12/15-LOX pathways

This was conducted as we did previously [1–3]. Briefly, 12*S*-HETE and 15*S*-HETE were extracted from mouse skin with methanol. The extract was cleaned up with a C18 solid phase extraction cartridge (500 mg), then analyzed using aqueous reversed-phase chiral liquid chromatography-ultra-violet spectrometer-LTQ tandem mass spectrometer (aR chiral LC-UV-MS/MS) coupled with a Chiralpak-IA-based chiral column (200 mm long × 2.1 mm ID × 5 μm).

Results

H&E staining revealed a delayed recovery of skin morphology after incision in 12/15-LOX$^{-/-}$ mice (Fig. 1). At 3 dpw, the cells were less dense in the wounded dermis of 12/15-

LOX$^{-/-}$ mice compared with WT mice (Fig. 1a and b). At 8 dpw, the re-epithelialization over the wound was obviously more in WT mice than that of 12/15-LOX$^{-/-}$ mice (Fig. 1c,d). At 14 dpw, the newly formed epidermis over wounds of WT appeared to have normal thickness and layers of cells; however the newly formed epidermis over wounds of 12/15-LOX$^{-/-}$ mice was thickened with more layers of cells (Fig. 1e,f). Therefore, our study provides evidence that 12/15-LOX$^{-/-}$ is detrimental for the recovery of skin morphology altered by wounding.

MSCs were determined in the wounded skin by immunohistological co-staining and microscope imaging of MSC makers Sca1 and CD29 (Fig. 2a–f,i), or Sca1 and CD106 (Fig. 3a–f,i), which is based on the reported flow cytometrical identification of MSCs using these markers[22,24]. There were more Sca1^{+}CD29^{+}MSCs (cells/field) at 3 (6.6 versus 3.0 MSCs/HPF, *$p < 0.05$), 8 (7.3 versus 4.6 MSCs/HPF, *$p < 0.05$), and 14 (11.6 versus 5.3 MSCs/HPF, **$p < 0.01$) dpw for WT mice compared to 12/15-LOX$^{-/-}$ mice (Fig. 2c–f). There were also more Sca1^{+}CD106^{+} MSCs in the wounded dermis of WT mice compared to 12/15-LOX$^{-/-}$ mice at 3 (5.0 versus 3.0 MSCs/HPF, *$p < 0.05$) and 14 (12.8 versus 5.8 MSCs/HPF, **$p < 0.01$) dpw (Figs. 3a,b,e,f,i), but the difference was not statistically significant at 8 dpw (Fig. 3c,d,i). It is interesting to note that there also was more MSCs in the dermis of wild type mice compared to 12/15-LOX$^{-/-}$ mice in sham condition (unwounded) (Figs. 2g–i, 3g–i). Compared to sham mice more Sca1^{+}CD29^{+} MSCs were found in the dermis of wounded skin at 3, 8 and 14 dpw in either wild type or 12/15-LOX$^{-/-}$ mice (Fig. 2). This trend also was observed for Sca1^{+}CD106^{+} MSCs (Fig. 3).

The kinetics of MSC densities in the wounded dermis of WT mice is different from 12/15-LOX$^{-/-}$ mice. For WT mice, more Sca1^{+}CD29^{+} MSCs homed in the wounded dermis at 14 dpw compared to 8 dpw (11.6 versus 7.3 MSCs/HPF, $p < 0.05$), but there was only a slight increase from 3 dpw to 8 dpw (Fig. 2i). For 12/15-LOX$^{-/-}$ wounded dermis, the increase of Sca1^{+}CD29^{+} MSCs from 3 to 8 dpw or from 8 to 14 dpw was not significant, but the increase of Sca1^{+}CD29^{+} MSCs from 3 to 14 dpw was significant (Fig. 2i). For 12/15-LOX$^{-/-}$ wounded dermis, Sca1^{+}CD106^{+}MSCs peaked at 8 dpw (7.5 versus 5.8 MSCs/HPF, $p < 0.05$ for 8 versus 14 dpw; 7.5 versus 3.0 MSCs/HPF, $p < 0.05$ for 8 versus 3 dpw). However for WT wounded dermis, MSCs increased from 3 dpw to 8 dpw (5.0 versus 9.0 MSCs/HPF, $p < 0.05$) and from 8 to 14 dpw (9.0 versus 12.8 MSCs/HPF, $p < 0.05$) (Fig. 3).

To further determine the difference between Sca1^{+}CD29^{+} MSCs and Sca1^{+}CD106^{+} MSCs, we conducted statistical analysis to compare these two MSC populations localized in the dermis (Figs. 2–4). It was found that there were significantly more Sca1^{+}CD29^{+} MSCs than Sca1^{+}CD106^{+} MSCs in wounded dermis of C57BL/6 mice (6.6 versus 5.0 MSCs/HPF, *$p < 0.05$) at 3 dpw (Fig. 4a), but more Sca1^{+}CD106^{+} MSCs than Sca1^{+}CD29^{+} MSCs in the wounded dermis of 12/15-LOX$^{-/-}$ mice (7.5 versus 4.6 MSCs/HPF, *$p < 0.05$) at 8 dpw (Fig. 4b). The difference of cell densities between Sca1^{+}CD106^{+} MSCs and Sca1^{+}CD29^{+} MSCs at other conditions was not significant (Fig. 4).

The significant impediment on MSC densities in incisional wounds of 12/15-LOX$^{-/-}$ mice (Figs. 2 and 3) suggests the suppression of 12/15-LOX product generation even though other LOXs could compensate the lost 12/15-LOX enzymatic capacity in 12/15-LOX$^{-/-}$ mice. To

test this prediction, we analyzed typical 12/15-LOX products in wounds of 12/15-LOX$^{-/-}$ and WT control mice in addition to our prior reported results[2] using aR-chiral LC-UV-MS/MS. 12*S*-HETE was well separated from 12*R*-HETE by the aR chiral LC (Fig. 5a). 12*S*-HETE and 15*S*-HETE were identified based on their MS/MS (Fig. 5B) and UV (Fig. 5b inset) spectra and LC chromagraphic retention times (Fig. 5a). The quantification shows that 12*S*-HETE, 15*S*-HETE and 17*S*-HDHA were reduced in wounds of 12/15-LOX$^{-/-}$ mice compared with the WT control (Fig. 5a,c). However, 12/15-LOX$^{-/-}$ did not have effect on arachidonic acid (AA) level in wounds (Fig. 5c right). The deficiency of 15*S*-HETE and 12*S*-HETE and other 12/15-LOX products are likely to be responsible for the reduced MSC densities in wounds of 12/15-LOX$^{-/-}$ mice.

12/15-LOX protein in WT wounded skin peaked at 3 dpw and remained higher at 8 and 14 dpws compared to unwounded skin (Fig. 6). The weak positive staining of the 12/15-LOX in 12/15-LOX$^{-/-}$ skin might result from the weak binding of antibody to protein trace expressed due to residual transcriptional activity of the 12/15-LOX neomycin cassette-disrupted allele, as pointed out by another group[27], or from the weak cross-reaction of antibody with other LOXs. The 12/15-LOX staining in 12/15-LOX−/− skin was much weaker than that of WT skin, indicating that the 12/15-LOX knockout diminished the 12/15-LOX expression (Fig. 6).

Discussion

Endogenous or transplanted MSCs home in skin wounds play an important role in healing. Therefore, MSC densities is critical for wound repair, as its impairment leads to chronic wounds.[23,28–31] Mechanisms that regulate MSC densities in skin are still largely unknown, which limits the harnessing of MSCs for clinical application. 12/15-LOX is one of the major enzymes that catalyzes the key steps of biosynthesis pathways to generate lipid mediators in wound healing[1,2,6,7,11,12]. Skin wound healing impaired by 12/15-LOX$^{-/-}$ [2] may involve suppressed densities of pro-healing MSCs. Our experimental results support this prediction: **1)** 12/15-LOX$^{-/-}$ reduces MSC densities in the wounded dermis; there were more Sca1^{+}CD29^{+}MSCs (cells/field) in the inflammation phase (at 3 dpw) and proliferation phase of wound healing (at 8 dpw) as well as between late proliferation and early remodeling phases of wound healing (at 14 dpw) and more Sca1^{+}CD106^{+}MSCs at 3 and 14 dpw in the wounded dermis of WT mice compared to 12/15-LOX$^{-/-}$ mice. **2)** The 12/15-LOX$^{-/-}$ alters the kinetics of MSC densities in the wounded dermis. Densities of Sca1^{+}CD29^{+} or Sca1^{+}CD106^{+}MSCs increases from the inflammation phase (at 3 dpw), proliferation phase, to the time between late proliferation and early remodeling phases in wounded WT dermis; however in wounded 12/15-LOX$^{-/-}$ dermis, Sca1^{+}CD29^{+}MSCs stayed at a comparable level during these phases, and Sca1^{+}CD106^{+}MSCs peaked in the proliferation phase (at 8 dpw) (Figs. 2,3). **3)** 12/15-LOX$^{-/-}$ alters the ratio between Sca1^{+}CD29^{+} and Sca1^{+}CD106^{+}MSCs in the inflammation phase (at 3 dpw) and proliferation phase of wound healing (at 8 dpw). It is interesting to note that the kinetics of endogenous MSC densities are different from leukocytes in wound healing[21]. For example, neutrophils reach the maximum number at ~1 dpw, at ~3 dpw for macrophages, and at 5 dpw for lymphocytes[21]. This reflects that the different functions of MSCs from leukocytes. Leukocytes protect wounds from infection of bacteria, fungi, and other microbes as well as remove dead cells and tissue

debris [21]. However, MSCs produce paracrines and replenish the loss cells in wounds[2,18–22]. To the best of our knowledge, this is the first report showing the impact of 12/15-LOX deficiency on MSC densities in the dermis during wound healing. These consequences of 12/15-LOX$^{-/-}$ on MSC densities may be responsible, at least partially, for the cutaneous healing defects of 12/15-LOX$^{-/-}$ mice [2,3,18#–22].

CD29 or integrin β1 play an important role in cell migration[32–34], suggesting that it may also function in the migration of CD29^{+} MSCs. The CD29 and the cell surface heterodimers formed from the interaction of CD29 with α4 integrins, involve in MSC mobilization, migration, and homing in the bone[35–38]. The CD29 deficiency reduces the rate of wound closure, decreases myofibroblast population and collagen deposition, and impairs cutaneous tissue repair *in vivo*[39], which may involve effects of CD29 deficiency on MSCs. Thus CD29 could function in MSC homing in wounded dermis, and Scal^{+}CD29^{+}MSCs could contribute to wound healing. CD106 or VCAM-1 is a cell adhesion molecule. MSCs act on the function of T cells, B cells, dendritic cells and NK cells in terms of immunomodulation[40]. These processes occur through cell-cell and cell-ECM communication connected through adhesion molecules including CD106[40]. Therefore Scal^{+}CD106^{+}MSCs could function in immunomodulation. 12/15-LOX could affect the immunomodulation executed by MSCs by regulating the homing of Sca1^{+}CD106^{+}MSCs to dermis and consequent densities of these cells. There were more Sca1^{+}CD106^{+}MSCs than Sca1^{+}CD29^{+}MSCs in 12/15-LOX$^{-/-}$ wounded dermis at 8 dpw, but less Sca1^{+}CD106^{+}MSCs than Sca1^{+}CD29^{+}MSCs in WT wounded dermis at 3 dpw.

LOXs in human and mouse skin include 5-LOX, platelet type 12-LOX (p12-LOX), 12/15-LOXs and epidermis-type LOXs (e12*S*-LOX, 12*R*-LOX, 8-LOX, eLOX-3)[5]. They are as follows: **1)** 5-LOX catalyzes the biosynthesis of leukotrienes, lipoxins, and resolvins[5–7]. It exists mainly in cells of myeloid origin including skin Langerhans cells[41]. While 5-LOX may not be critical in skin homeostasis[42], but it functions in diseases because leukotrienes act in psoriasis and atopic dermatitis[43,44]; lipoxins and resolvins function in resolving the inflammation[5–7], and leukotriene B_4 induce keratinocyte proliferation[5,45]. **2)** 8-LOX is in mouse cutaneous adnexa, hair follicles, and most abundantly in skin glands[46]. 8-LOX produces the precursor of 8*S*-HETE. 8*S*-HETE may stimulate differentiation of keratinocytes[47]. **3)** 12/15-LOXs include leukocyte-type 12-LOX (l12-LOX) in leukocytes and human reticulocyte-type 15-LOX-1. 12/15-LOXs have a dual positional specificity oxygenating AA to both 12*S*- and 15*S*-hydroperoxy-eicosatetraenoic-acid (HpETE), linoleic acid to 13*S*-hydroperoxy octadecadienoic acid (HpODE), and DHA to 14*S*- and 17*S*-hydroperoxy DHAs (HpDHA). 12/15-LOX also oxygenates esterified PUFAs[48]. This oxygenation is the key step producing lipid mediators with diversified functions[2,6,7,11,12], which is outlined in the Scheme. 12/15-LOXs express strongly in macrophages[49], human reticulocytes and eosinophils, but weakly in adipose tissue[5]. They also exist in epidermal keratinocytes[50]. **4)** Platelets, epidermal keratinocytes, and leukocytes express p12-LOX[50–52]. The p12-LOX oxygenates AA to 12*S*-HpETE and DHA to 14*S*-HpDHA[53], and linoleic acid less efficiently to 13*S*-HpODE[54,55]. The p12-LOX has no role in epidermal barrier function[56], but it may play a role in proliferation and differentiation of keratinocytes via its product 12*S*-HETE[57]. **5)** The e12*S*-LOX expresses in the epidermis, hair follicles, and

sebaceous glands[58]. It has a dual 12/15-LOX specificitywith low reactivity (inactive on DHA)[55,59,60]. Its bioaction is unclear. **6)** Human 12*R*-LOX converts AA to 12*R*-HpETE and converts few other PUFAs at the ω-9 position with poor efficiency[61]. Mouse 12*R*-LOX is inactive on AA or DHA, but active on AA methyl ester[60,61]. 12*R*-LOX-produced produce hydroxyceramide-derivative constitutes skin cornified envelope for skin barrier function[5,62]. **7)** The eLOX-3 transforms 12HpETEsto hepoxilins and or several other PUFA hydroperoxides to hepoxilins-like compounds[63]. Skin deficient of eLOX-3 has reduced levels of hepoxilin metabolites[5]. Hepoxilins and their hydrolysis products function in inflammation[12]. Moreover eLOX-3-produced ceramide-derivatives are crucial to form cornified envelope[5]. 12*R*-LOX and eLOX-3 exist at the surface of the keratinocytes of mouse skin[64]. Taken together, 12/15-LOXs are different from other LOXs for their oxygenation positional specificity, substrate preference, and/or specific localization in skin, which could be responsible for their indispensable role in MSC functions, indicated by our observation on significant suppression effects of 12/15-LOX$^{-/-}$ on MSC densities in the dermis.

Wounding-induced increase of 12/15-LOX expression represents a reparative response, since higher 12/15-LOX levels correspond to the increased densities of pro-healing MSCs (Figs. 2–4,6). 12/15-LOX in WT unwounded skin was significantly higher than that in 12/15-LOX$^{-/-}$ unwounded skin, which was correlated with more MSCs in the WT unwounded dermis compared to 12/15-LOX$^{-/-}$ mice (Figs. 2,3,6). This suggests that 12/15-LOX contributes the maintenance of the endogenous MSCs for dermis homeostasis. The 12/15-LOX$^{-/-}$ reduces the levels of 12*S*-HETE and 15*S*-HETE, indicating the suppression of oxygenation in C_{12} and C_{15} positions of AA in wounds, respectively (Fig. 5). In parallel, it also reduces levels of 14*S*-HDHA and 17*S*-HDHA, which shows that there is a decrease of oxygenation in C_{14} and C_{17} positions of DHA in wounds, respectively. The p12-LOX could also oxygenate AA at C_{12} and DHA at C_{14}, and e12*S*-LOX could oxygenate AA at C_{12} with very low efficiency. However our data show that these skin enzymes do not compensate the suppression of 12*S*-HETE, 15*S*-HETE, 14*S*-HDHA, and 17*S*-HDHA in wounds caused by 12/15-LOX$^{-/-}$ (Fig. 5). This is consistent with the significant suppressive effects of 12/15-LOX$^{-/-}$ on 12/15-LOX expression and MSC densities in the dermis of cutaneous wounds, which also are not compensated by other LOXs in wounds. Our results suggest that the suppressed MSC population in the wounded and unwounded dermis of 12/15-LOX$^{-/-}$ mice could result from the deficiency-caused suppression of lipid mediators produced in these oxygenation pathways including 12*S*-HETE, 15*S*-HETE, 13*S*-HODE, 17*S*-HDHA, 14*S*,21*R*-diHDHA, neuroptectin D1, resolvins D1 to D6, lipoxin A_4, and lipoxin B_4[4,65]. These products may combine and synergize with each other to promote MSC densities in the wounded dermis and/or maintain MSCs in unwounded dermis. Identification of the exact 12/15-LOX-produced lipid mediators regulating MSC homing and density is of interest for our future study. Moreover the effects of 12/15-LOX deficiency on MSC homing and density in the epidermis and hypodermis also need to be studied in the future.

Acknowledgments

This work is supported by NIH grant R01-DK087800 (S.H.). We thank Drs. Nicolas G. Bazan and Haydee E.P. Bazan (Neuroscience Center of Excellence at the Louisiana State University Health Sciences Center, New Orleans, LA) for the 12/15-LOX knockout mice. Many thanks to Mr. Ryan Labadens for his editorial assistance.

References

1. Lu Y, Tian H, Hong S. Novel 14,21-dihydroxy-docosahexaenoic acids: structures, formation pathways, and enhancement of wound healing. J Lipid Res. 2010; 51:923–32. [PubMed: 19965612]
2. Tian H, Lu Y, Shah SP, et al. 14S,21R-Dihydroxydocosahexaenoic Acid Remedies Impaired Healing and Mesenchymal Stem Cell Functions in Diabetic Wounds. J Biol Chem. 2011; 286:4443–53. [PubMed: 21112969]
3. Tian H, Lu Y, Shah SP, et al. Autacoid 14S,21R-dihydroxy-docosahexaenoic acid counteracts diabetic impairment of macrophage prohealing functions. Am J Pathol. 2011; 179:1780–91. [PubMed: 21839062]
4. Serhan CN, Petasis NA. Resolvins and protectins in inflammation resolution. Chem Rev. 2011; 111:5922–43. [PubMed: 21766791]
5. Krieg P, Furstenberger G. The role of lipoxygenases in epidermis. Biochim Biophys Acta. 2013
6. Serhan CN, Hong S, Gronert K, et al. Resolvins: a family of bioactive products of omega-3 fatty acid transformation circuits initiated by aspirin treatment that counter proinflammation signals. J Exp Med. 2002; 196:1025–37. [PubMed: 12391014]
7. Hong S, Gronert K, Devchand PR, et al. Novel docosatrienes and 17S-resolvins generated from docosahexaenoic acid in murine brain, human blood, and glial cells. Autacoids in anti-inflammation. J Biol Chem. 2003; 278:14677–87. [PubMed: 12590139]
8. Marcheselli VL, Hong S, Lukiw WJ, et al. Novel docosanoids inhibit brain ischemia-reperfusion-mediated leukocyte infiltration and pro-inflammatory gene expression. J Biol Chem. 2003; 278:43807–17. [PubMed: 12923200]
9. Gronert K, Maheshwari N, Khan N, et al. A role for the mouse 12/15-lipoxygenase pathway in promoting epithelial wound healing and host defense. J Biol Chem. 2005; 280:15267–78. [PubMed: 15708862]
10. Uderhardt S, Kronke G. 12/15-lipoxygenase during the regulation of inflammation, immunity, and self-tolerance. J Mol Med (Berl). 2012; 90:1247–56. [PubMed: 22983484]
11. Profita M, Sala A, Siena L, et al. Leukotriene B4 production in human mononuclear phagocytes is modulated by interleukin-4-induced 15-lipoxygenase. J Pharmacol Exp Ther. 2002; 300:868–75. [PubMed: 11861792]
12. Pace-Asciak CR. The hepoxilins and some analogues: a review of their biology. Br J Pharmacol. 2009; 158:972–81. [PubMed: 19422397]
13. Kenchegowda S, Bazan NG, Bazan HE. EGF stimulates lipoxin A4 synthesis and modulates repair in corneal epithelial cells through ERK and p38 activation. Invest Ophthalmol Vis Sci. 2011; 52:2240–9. [PubMed: 21220563]
14. Calandria JM, Marcheselli VL, Mukherjee PK, et al. Selective survival rescue in 15-lipoxygenase-1-deficient retinal pigment epithelial cells by the novel docosahexaenoic acid-derived mediator, neuroprotectin D1. J Biol Chem. 2009; 284:17877–82. [PubMed: 19403949]
15. Jiang Y, Jahagirdar BN, Reinhardt RL, et al. Pluripotency of mesenchymal stem cells derived from adult marrow. Nature. 2002; 418:41–9. [PubMed: 12077603]
16. Liu JW, Dunoyer-Geindre S, Serre-Beinier V, et al. Characterization of endothelial-like cells derived from human mesenchymal stem cells. J Thromb Haemost. 2007; 5:826–34. [PubMed: 17229052]
17. Wang X, Hisha H, Taketani S, et al. Characterization of mesenchymal stem cells isolated from mouse fetal bone marrow. Stem Cells. 2006; 24:482–93. [PubMed: 16179426]
18. Javazon EH, Keswani SG, Badillo AT, et al. Enhanced epithelial gap closure and increased angiogenesis in wounds of diabetic mice treated with adult murine bone marrow stromal progenitor cells. Wound Repair Regen. 2007; 15:350–9. [PubMed: 17537122]

19. Wu Y, Chen L, Scott PG, et al. Mesenchymal stem cells enhance wound healing through differentiation and angiogenesis. Stem Cells. 2007; 25:2648–59. [PubMed: 17615264]
20. Stepanovic V, Awad O, Jiao C, et al. Leprdb diabetic mouse bone marrow cells inhibit skin wound vascularization but promote wound healing. Circ Res. 2003; 92:1247–53. [PubMed: 12730094]
21. Broughton G 2nd, Janis JE, Attinger CE. The basic science of wound healing. Plast Reconstr Surg. 2006; 117:12S–34S. [PubMed: 16799372]
22. Chen L, Tredget EE, Wu PY, et al. Paracrine factors of mesenchymal stem cells recruit macrophages and endothelial lineage cells and enhance wound healing. PLoS ONE. 2008; 3:e1886. [PubMed: 18382669]
23. Albiero M, Menegazzo L, Boscaro E, et al. Defective recruitment, survival and proliferation of bone marrow-derived progenitor cells at sites of delayed diabetic wound healing in mice. Diabetologia. 2011; 54:945–53. [PubMed: 21165593]
24. Rostovskaya M, Anastassiadis K. Differential expression of surface markers in mouse bone marrow mesenchymal stromal cell subpopulations with distinct lineage commitment. PLoS One. 2012; 7:e51221. [PubMed: 23236457]
25. Tobita M, Orbay H, Mizuno H. Adipose-derived stem cells: current findings and future perspectives. Discov Med. 2011; 11:160–70. [PubMed: 21356171]
26. Tian H, Lu Y, Shah SP, et al. Novel 14S,21-dihydroxy-docosahexaenoic acid rescues wound healing and associated angiogenesis impaired by acute ethanol intoxication/exposure. J Cell Biochem. 2010; 111:266–73. [PubMed: 20506249]
27. Poeckel D, Zemski Berry KA, Murphy RC, et al. Dual 12/15- and 5-lipoxygenase deficiency in macrophages alters arachidonic acid metabolism and attenuates peritonitis and atherosclerosis in ApoE knock-out mice. J Biol Chem. 2009; 284:21077–89. [PubMed: 19509298]
28. Velazquez OC. Angiogenesis and vasculogenesis: inducing the growth of new blood vessels and wound healing by stimulation of bone marrow-derived progenitor cell mobilization and homing. J Vasc Surg. 2007; 45(Suppl A):A39–47. [PubMed: 17544023]
29. Tepper OM, Carr J, Allen RJ Jr. et al. Decreased circulating progenitor cell number and failed mechanisms of stromal cell-derived factor-1alpha mediated bone marrow mobilization impair diabetic tissue repair. Diabetes. 2010; 59:1974–83. [PubMed: 20484135]
30. Kim KA, Shin YJ, Kim JH, et al. Dysfunction of endothelial progenitor cells under diabetic conditions and its underlying mechanisms. Arch Pharm Res. 2012; 35:223–34. [PubMed: 22370777]
31. Cianfarani F, Toietta G, Di Rocco G, et al. Diabetes impairs adipose tissue-derived stem cell function and efficiency in promoting wound healing. Wound Repair Regen. 2013
32. Ip JE, Wu Y, Huang J, et al. Mesenchymal stem cells use integrin beta1 not CXC chemokine receptor 4 for myocardial migration and engraftment. Mol Biol Cell. 2007; 18:2873–82. [PubMed: 17507648]
33. Hynes RO. Integrins: bidirectional, allosteric signaling machines. Cell. 2002; 110:673–87. [PubMed: 12297042]
34. De Ugarte DA, Alfonso Z, Zuk PA, et al. Differential expression of stem cell mobilization-associated molecules on multi-lineage cells from adipose tissue and bone marrow. Immunol Lett. 2003; 89:267–70. [PubMed: 14556988]
35. Guan JL, Hynes RO. Lymphoid cells recognize an alternatively spliced segment of fibronectin via the integrin receptor alpha 4 beta 1. Cell. 1990; 60:53–61. [PubMed: 2295088]
36. Schweitzer KM, Drager AM, van der Valk P, et al. Constitutive expression of E-selectin and vascular cell adhesion molecule-1 on endothelial cells of hematopoietic tissues. Am J Pathol. 1996; 148:165–75. [PubMed: 8546203]
37. Jacobsen K, Kravitz J, Kincade PW, et al. Adhesion receptors on bone marrow stromal cells: in vivo expression of vascular cell adhesion molecule-1 by reticular cells and sinusoidal endothelium in normal and gamma-irradiated mice. Blood. 1996; 87:73–82. [PubMed: 8547679]
38. Jin H, Aiyer A, Su J, et al. A homing mechanism for bone marrow-derived progenitor cell recruitment to the neovasculature. J Clin Invest. 2006; 116:652–62. [PubMed: 16498499]
39. Liu S, Xu SW, Blumbach K, et al. Expression of integrin beta1 by fibroblasts is required for tissue repair in vivo. J Cell Sci. 2010; 123:3674–82. [PubMed: 20940256]

40. Nauta AJ, Fibbe WE. Immunomodulatory properties of mesenchymal stromal cells. Blood. 2007; 110:3499–506. [PubMed: 17664353]
41. Haeggstrom JZ, Funk CD. Lipoxygenase and leukotriene pathways: biochemistry, biology, and roles in disease. Chem Rev. 2011; 111:5866–98. [PubMed: 21936577]
42. Funk CD, Chen XS, Johnson EN, et al. Lipoxygenase genes and their targeted disruption. Prostaglandins Other Lipid Mediat. 2002; 68–69:303–12.
43. Ruzicka T, Simmet T, Peskar BA, et al. Skin levels of arachidonic acid-derived inflammatory mediators and histamine in atopic dermatitis and psoriasis. J Invest Dermatol. 1986; 86:105–8. [PubMed: 3018086]
44. Ohnishi H, Miyahara N, Gelfand EW. The role of leukotriene B(4) in allergic diseases. Allergol Int. 2008; 57:291–8. [PubMed: 18797182]
45. Reusch MK, Wastek GJ. Human keratinocytes in vitro have receptors for leukotriene B4. Acta Derm Venereol. 1989; 69:429–31. [PubMed: 2572111]
46. Shappell SB, Keeney DS, Zhang J, et al. 15-Lipoxygenase-2 expression in benign and neoplastic sebaceous glands and other cutaneous adnexa. J Invest Dermatol. 2001; 117:36–43. [PubMed: 11442747]
47. Muga SJ, Thuillier P, Pavone A, et al. 8S-lipoxygenase products activate peroxisome proliferator-activated receptor alpha and induce differentiation in murine keratinocytes. Cell Growth Differ. 2000; 11:447–54. [PubMed: 10965849]
48. Kuhn H, O'Donnell VB. Inflammation and immune regulation by 12/15-lipoxygenases. Prog Lipid Res. 2006; 45:334–56. [PubMed: 16678271]
49. Heidt M, Furstenberger G, Vogel S, et al. Diversity of mouse lipoxygenases: identification of a subfamily of epidermal isozymes exhibiting a differentiation-dependent mRNA expression pattern. Lipids. 2000; 35:701–7. [PubMed: 10941870]
50. Zhao H, Richards-Smith B, Baer AN, et al. Lipoxygenase mRNA in cultured human epidermal and oral keratinocytes. J Lipid Res. 1995; 36:2444–9. [PubMed: 8656082]
51. Holtzman MJ, Turk J, Pentland A. A regiospecific monooxygenase with novel stereopreference is the major pathway for arachidonic acid oxygenation in isolated epidermal cells. J Clin Invest. 1989; 84:1446–53. [PubMed: 2509517]
52. Takahashi Y, Reddy GR, Ueda N, et al. Arachidonate 12-lipoxygenase of platelet-type in human epidermal cells. J Biol Chem. 1993; 268:16443–8. [PubMed: 8344930]
53. Kim HY, Karanian JW, Shingu T, et al. Stereochemical analysis of hydroxylated docosahexaenoates produced by human platelets and rat brain homogenate. Prostaglandins. 1990; 40:473–90. [PubMed: 2147773]
54. Funk CD, Furci L, FitzGerald GA. Molecular cloning, primary structure, and expression of the human platelet/erythroleukemia cell 12-lipoxygenase. Proc Natl Acad Sci U S A. 1990; 87:5638–42. [PubMed: 2377602]
55. Burger F, Krieg P, Marks F, et al. Positional- and stereo-selectivity of fatty acid oxygenation catalysed by mouse (12S)-lipoxygenase isoenzymes. Biochem J. 2000; 348(Pt 2):329–35. [PubMed: 10816426]
56. Johnson EN, Nanney LB, Virmani J, et al. Basal transepidermal water loss is increased in platelet-type 12-lipoxygenase deficient mice. J Invest Dermatol. 1999; 112:861–5. [PubMed: 10383730]
57. Hagerman RA, Fischer SM, Locniskar MF. Effect of 12-O-tetradecanoylphorbol-13-acetate on inhibition of expression of keratin 1 mRNA in mouse keratinocytes mimicked by 12(S)-hydroxyeicosatetraenoic acid. Mol Carcinog. 1997; 19:157–64. [PubMed: 9254882]
58. Funk CD, Keeney DS, Oliw EH, et al. Functional expression and cellular localization of a mouse epidermal lipoxygenase. J Biol Chem. 1996; 271:23338–44. [PubMed: 8798535]
59. McDonnell M, Davis W Jr. Li H, et al. Characterization of the murine epidermal 12/15-lipoxygenase. Prostaglandins Other Lipid Mediat. 2001; 63:93–107. [PubMed: 11204741]
60. Siebert M, Krieg P, Lehmann WD, et al. Enzymic characterization of epidermis-derived 12-lipoxygenase isoenzymes. Biochem J. 2001; 355:97–104. [PubMed: 11256953]
61. Boeglin WE, Kim RB, Brash AR. A 12R-lipoxygenase in human skin: mechanistic evidence, molecular cloning, and expression. Proc Natl Acad Sci U S A. 1998; 95:6744–9. [PubMed: 9618483]

62. Zheng Y, Yin H, Boeglin WE, et al. Lipoxygenases mediate the effect of essential fatty acid in skin barrier formation: a proposed role in releasing omega-hydroxyceramide for construction of the corneocyte lipid envelope. J Biol Chem. 2011; 286:24046–56. [PubMed: 21558561]

63. Yu Z, Schneider C, Boeglin WE, et al. Human and mouse eLOX3 have distinct substrate specificities: implications for their linkage with lipoxygenases in skin. Arch Biochem Biophys. 2006; 455:188–96. [PubMed: 17045234]

64. Epp N, Furstenberger G, Muller K, et al. 12R-lipoxygenase deficiency disrupts epidermal barrier function. J Cell Biol. 2007; 177:173–82. [PubMed: 17403930]

65. Bazan NG. Homeostatic regulation of photoreceptor cell integrity: significance of the potent mediator neuroprotectin D1 biosynthesized from docosahexaenoic acid: the Proctor Lecture. Invest Ophthalmol Vis Sci. 2007; 48:4866–81. biography 4–5. [PubMed: 17962433]

What's already known about this topic?

Mesenchymal stem cells (MSCs) are known to be recruited to wounded skin and promote healing. 12/15-lipoxgenase and its products are present in the skin. 12/15-lipoxygenase deficiency suppresses wound healing.

What does this study add?

We have discovered for the first time that 12/15-lipoxygenase deficiency reduces MSC densities in the dermis of wounded and unwounded skin.

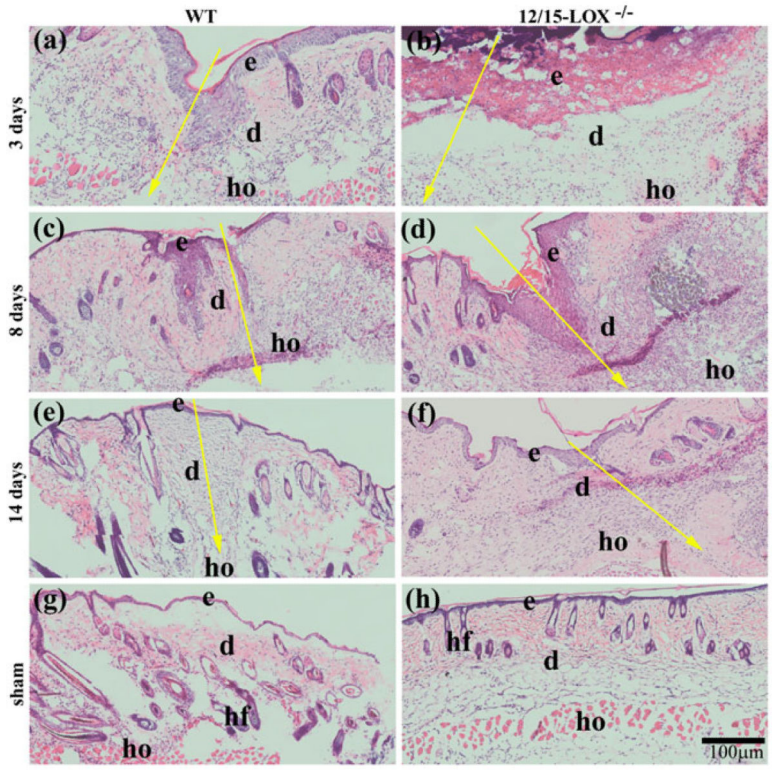

Fig. 1. Impaired recovery of skin morphology occurs in 12/15-LOX$^{-/-}$ mice after incisional wounding

(a–f) Wounded and (g–h) unwounded (sham) skin sections were stained by hematoxylin and eosin (HE). Incisional wounding was conducted on 12/15-LOX$^{-/-}$ and congenic wildtype (WT) control mice (C57BL/6) and skin samples were collected at 3, 8, and 14 days post-wounding (dpw). Images (a), (c), (e) and (f) were acquired from the skin of WT mice; Images (b), (d), (f) and (h) were acquired from the skin of 12/15-LOX$^{-/-}$ mice. 12/15-LOX$^{-/-}$ impaired the recovery of skin morphology damaged by wounding. e, epidermis; d, dermis; hf, hair follicle; ho, hypodermis; Big yellow arrow, the incisional wound (a–f) and direction of skin layers from epidermis to hypodermis; Scale bar = 100 μm.

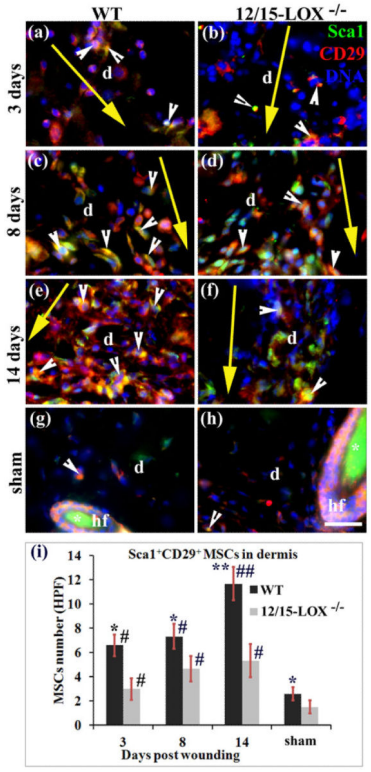

Fig. 2. 12/15-LOX deficiency reduces densities of Sca1^{+}CD29^{+} MSCs in the dermis of wounded skin

Images in (a) and (b), images in (c) and (d), and images in (e) and (f), are for 3, 8 and 14 dpw, respectively. Images in (g) and (h) are for sham (unwounded skin). Images in (a), (c), (e) and (g), and images in (b), (d), (f) and (h), are for C57BL/6 (WT) and 12/15-LOX$^{-/-}$ mice, respectively. Immunofluorescent co-staining and microscope imaging were conducted on cryosections of each wound with a 10 mm margin of surrounding skin, or skin at the equivalent location of sham. (i) There are more cells co-stained (yellow) for Sca1 and CD29 (i.e, Sca1^{+}CD29^{+} MSCs) in the wounded dermis of WT mice compared to 12/15-LOX$^{-/-}$ mice for 3, 8 and 14 dpw. Each value is the average number per HPF of Sca1^{+}CD29^{+} MSCs from six mice per group ± SD. *$p < 0.05$ and **$p < 0.01$ are for WT versus 12/15-LOX$^{-/-}$; #$p < 0.05$ and ##$p < 0.01$ are for the wounded versus sham of the same type of mice. HPF, high power field (63X); d, dermis; hf, hair follicle; Asterisk (*), unspecific binding of secondary antibody (g–h); Big yellow arrow, incisional wound and direction from epidermis to hypodermis of skin (a–f); Scale bar = 28 μm.

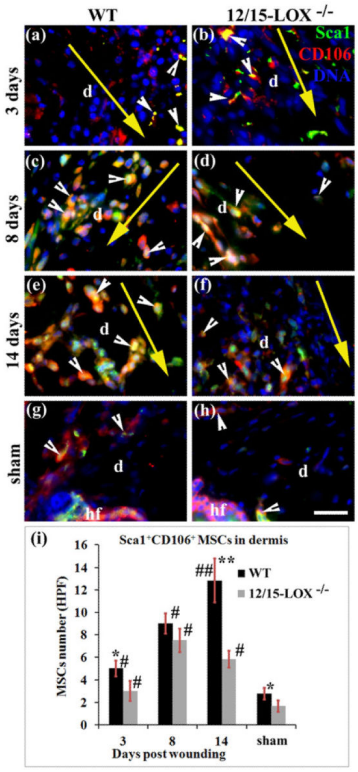

Fig. 3. 12/15-LOX deficiency reduces densities of Sca1^{+}CD106^{+} MSCs in the dermis of wounded skin

Images in (a) and (b), images in (c) and (d), and image (e) and (f), are for 3, 8 and 14 dpw, respectively. Images (g) and (h) are for sham. Images in (a), (c), (e) and (g), and images in (b), (d), (f) and (h), are for C57BL/6 (WT) and 12/15-LOX$^{-/-}$ mice, respectively. Immunofluorescent co-staining and microscope imaging were conducted on cryosections of each wound with 10 mm margin of surrounding skin, or skin at the equivalent location of sham. (i) There are more cells co-stained (yellow) of Sca1 and CD106 (i.e, Sca1^{+}CD106^{+} MSCs) in the wounded dermis of WT mice compared to 12/15-LOX$^{-/-}$ mice for 3, 8 and 14 days post-wounding. Each value is the average number per HPF of Sca1^{+}CD106^{+} MSCs from six mice per group ± SD. *p < 0.05 and **p < 0.01 are for WT versus 12/15-LOX$^{-/-}$ mice; #p < 0.05 and ##p < 0.01 are for the wounded versus sham of the same type of mice. HPF, high power field (63X); d, dermis; hf, hair follicle; Big yellow arrow, incisional wound and direction from epidermis to hypodermis of skin (a–f); Scale bar = 28 μm.

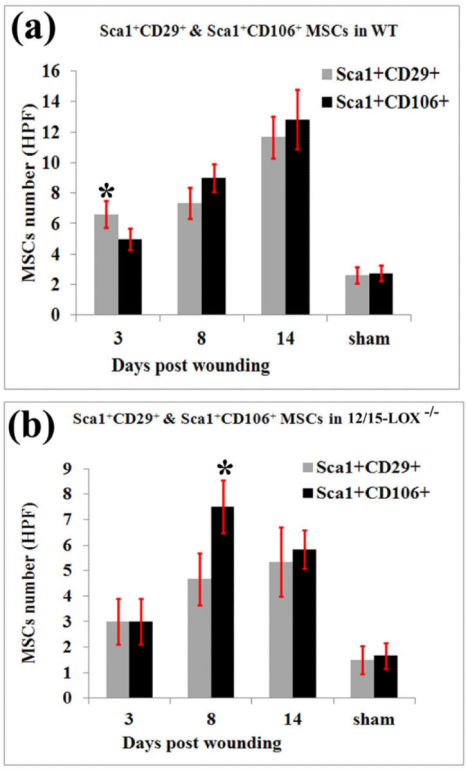

Fig. 4. Sca1^{+}CD106^{+}MSCs are more abundant than Sca1^{+}CD29^{+}MSCs in the 12/15-LOX$^{-/-}$ wounded dermis at 8 dpw, but less abundant in the WT wounded dermis at 3 dpw

(a) WT mice. (b) 12/15-LOX$^{-/-}$ mice. There were comparable cell densities in the dermis for each in other conditions. Each value is the average number per HPF of MSCs from six mice per group ± SD. *$p < 0.05$ are for Sca1^{+}CD106^{+} MSCs versus Sca1^{+}CD29^{+} MSCs.

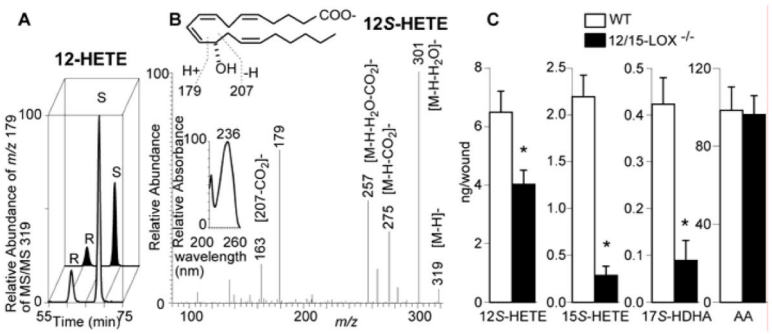

Fig. 5. 12/15-LOX deficiency reduces the wound levels of 12*S*-HETE, 15*S*-HETE, and 17*S*-HDHA, which represent the 12/15-LOX pathways in wounds

Samples of 3 dpw were analyzed by aR-chiral LC-UVMS/MS. (a) Typical chromatograms of 12*S*-HETE and 12*R*-HETE; (b) Typical UV (left inset) and MS/MS spectra with MS/MS-based structure elucidation (top inset) for 12*S*-HETE in the wounded skin of C57BL/6 mice; (c) Amount of 12*S*-HETE, 15*S*-HETE, 17*S*-HDHA and arachidonic acid (AA) in skin wounds (ng/wound). Data are reported as means ± SEM. (n = 3). *$p < 0.05$.

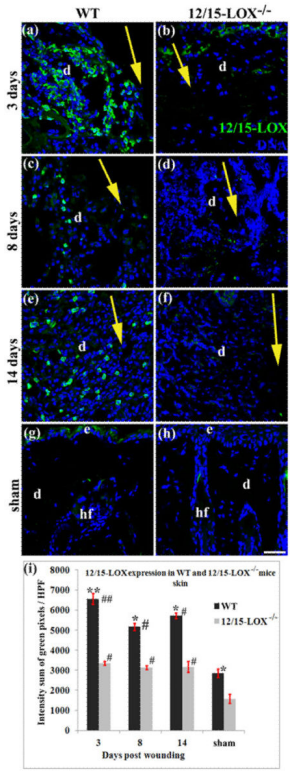

Fig. 6. 12/15-LOX expression in wounded and unwounded skin of 12/15-LOX$^{-/-}$ and WT mice

12/15-LOX in wounded and unwounded skin were measured by an immunofluorescent histological method. Images in (a) and (b), images in (c) and (d), and image in (e) and (f), are for 3, 8 and 14 dpw, respectively. Images in (g) and (h) are for sham (unwounded skin). Images in (a), (c), (e) and (g), and images in (b), (d), (f) and (h), are for C57BL/6 (WT) and 12/15-LOX$^{-/-}$ mice, respectively. (i) Intensity summation of green fluorescent pixels per HPF of 12/15-LOX stained skin sections. Each value is the average of four mice per group ± SD. *$p < 0.05$ and **$p < 0.01$ are for WT versus 12/15-LOX$^{-/-}$; #$p < 0.05$ and ##$p < 0.01$ are for the wounded versus sham of the same type of mice. Wound healing model or histological method was the same as in Fig 2. Nuclei are counterstained with DAPI (blue). HPF, high power field (40X); d, dermis; hf, hair follicle; Big yellow arrow, incisional wound and direction from epidermis to hypodermis of skin; Scale bar = 38 μm.

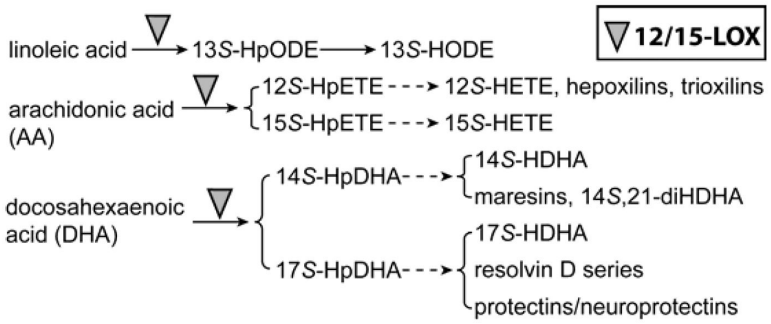

Scheme.

12/15-LOX-initiated biosynthetic pathways for key lipid mediators in wound niche of MSCs.